Anisotropic conductance oscillations in Pb films on Si(557)

D. Lükermann, H. Pfnür, and C. Tegenkamp
Institut für Festkörperphysik, Leibniz Universität Hannover, Appelstrasse 2, D-30167 Hannover, Germany
(Received 29 March 2010; revised manuscript received 14 May 2010; published 1 July 2010)

We correlate in this study the growth of Pb films on the stepped Si(557) surface at temperatures of 70 K, studied by low-energy electron diffraction, with the properties of electronic transport, measured by a macroscopic four-point probe technique. Despite a large lattice mismatch, layer-by-layer growth is observed, as most obvious from the characteristic oscillations in conductance with layer periodicity, incipient with the first monolayer both along and across the step direction. These findings demonstrate that lateral misfits (here almost 10%) in heteroepitaxial systems can be effectively compensated by substrate steps and can change the growth mode with respect to flat surfaces. While structurally the layers appear to be isotropic starting already with the third layer, anisotropy is seen in transport up to at least six monolayers with functional dependencies of conductance varying with layer thickness and measurement direction. Maxima of conductance oscillations up to five monolayers do not coincide with completion of individual layers. They are characteristic for the close coupling of structure and quantum effects.

DOI: 10.1103/PhysRevB.82.045401 PACS number(s): 68.55.J−, 73.50.−h, 73.61.−r

I. INTRODUCTION

Metallic thin films, and particularly monolayers, on semiconductor substrates are currently studied extensively because they seem to be adequate model systems for highly correlated low dimensional electron gases.[1–6] The main reason is that, although chemical bonds are formed at the interface, the topmost occupied electronic states mix with the surface states of the substrate and remain within the bulk band gaps. Thus for these states and for low-lying excitations, the substrate is electronically decoupled. This opens the possibility to investigate purely two-dimensional transport behavior as well as the transition to three dimensions by varying the layer thickness. These systems also allow a direct correlation of transport with the structure of the film.[7] It is obvious that interface effects such as lattice mismatch, strain effects, metal induced band-gap states, etc. must couple intimately with the electronic properties.

For example, the formation of quantum well states (QWS) as identified in spectroscopy for Pb layers on Si(111) (Refs. 8 and 9) directly modifies growth by stabilizing certain layer thicknesses (e.g., by formation of islands with "magic" heights) and is also measurable in conductance.[8–13] In this system at low temperatures the lattice mismatch of almost 10% results first in growth of an amorphous film but is converted into crystalline growth above four monolayers.[14] Oscillations of conductance with increasing film thickness have been found only in the recrystallization regime and were explained in terms of classical size effects (CSE). Precisely speaking, this variation is due to the varying effective roughness of the vacuum interface during growth, resulting in a varying fraction of specularly reflected electrons from the surface during growth. At the same time, this is a clear indication for layer-by-layer growth.[10,11] This surface effect is described by a specularity parameter within the Fuchs-Sondheimer model,[15,16] which is based on the Boltzmann transport equation. For ultrathin films the discrete energy-level spectrum becomes relevant even at room temperature, and this approach breaks down.

As seen from this example, stress-induced modifications of growth are crucial also for the transport properties, and in general strongly reduce conductance through such structures. On the other hand, lattice-matched systems are very rare. Therefore, possibilities for compensation of stress are of high importance. One promising strategy is the use of wetting layers. Particularly for the Pb/Si(111) system intermediate layers such as Au-6×6 or Pb-$\sqrt{3}\times\sqrt{3}$ reconstructions were used in order to trigger instantaneously a layer-by-layer growth.[13,17]

In the study described in this paper we stick to the combination of Pb on Si and investigate again the correlation between structure and lateral conductance but we now introduce a regular periodic arrangement of steps at the interface by use of a Si(557) surface. Contrary to the intuitive expectation, we show that these regularly arranged steps provide an important stress compensating mechanism that allows layer-by-layer growth from the beginning and also for thick layers. Nevertheless, the anisotropy of the interface is directly reflected in our thickness dependent conductance measurements, which allow direct conclusions about the scattering properties of the steps and their role within the layers both for conductance and growth. We focus on macroscopic four-point probe measurements of the conductance during growth of Pb layers on Si(557). The morphology is controlled by electron diffraction.

The paper is organized as follows: we first concentrate on structural properties as a function of layer thickness before turning to the conductive properties. Here the general functional dependence on layer thickness is described first before analyzing the thickness dependent conductance oscillations in detail and correlate them with the structure of the films.

II. EXPERIMENTAL SETUP

Low-doped Si(557) samples (15×15 mm^2 in size) with eight $TiSi_2$ contacts have been used to perform four-point probe conductance measurements, both parallel and perpendicular to the step directions of the Si(557) substrate. The

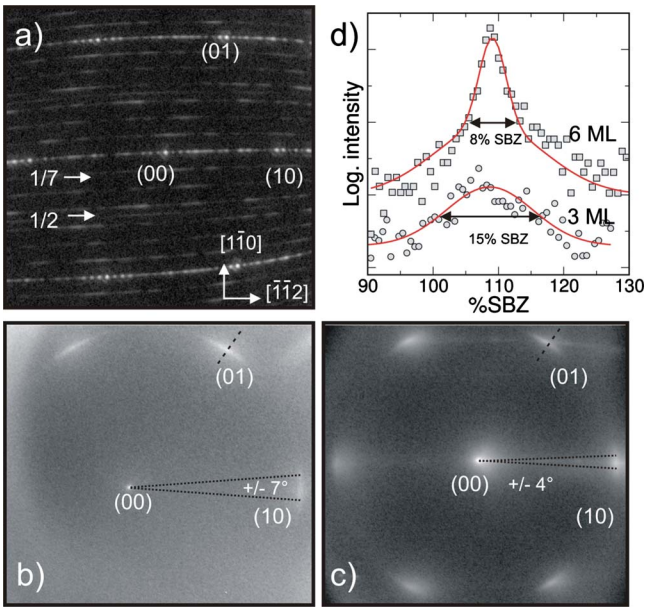

FIG. 1. (Color online) LEED patterns at a surface temperature of 70 K of clean Si(557) (a) after adsorption of 3 ML (b) and 6 ML of Pb (c) without further annealing. The electron energy was 96 eV. (d) Radial line scans taken along the dashed lines in (b) and (c). The dotted lines illustrate the azimuthal broadening of the Pb reflexes. Throughout the paper the inplane crystallographic directions are given with respect to the orientation of the mini-(111) terraces.

contacts were fabricated afore by evaporation of Ti on the hydrofloric acid (HF)-dipped samples in a vacuum of 10^{-4} Pa followed by annealing to around 700 °C for the silicide formation. Thereafter, the samples were mounted on the sample holder and transferred into the main UHV chamber (base pressure 1×10^{-8} Pa). Crystalline Si surfaces were obtained by subsequent flashing the samples by electron bombardment to temperatures around 1100 °C. The morphology was controlled by spot profile analysis low energy electron diffraction (SPA-LEED). Figure 1(a) shows a characteristic LEED pattern of a well prepared Si(557) surface. Pb was evaporated out of a ceramic crucible and the amount controlled by a quartz microbalance. The source itself was accurately calibrated by means of characteristic reconstructions in the submonolayer regime[18] as well as by oscillations in transport during Pb evaporation (see below). Since in this study the properties of multilayers are studied, the coverage is given with respect to physical monolayers throughout this paper. A He-flow cryostat together with an *in situ* radiation shield allowed continuous adjustment of sample temperatures between 4 K (with cooled radiation shield) and 300 K. The temperature was measured by a Si-diode mounted on the cryostat and was calibrated using thermocouples mounted directly on dummy samples.

III. RESULTS AND DISCUSSION

A. Structure and epitaxy

The main aim of this section is to show how quickly the anisotropy of the original Si(557) surface is washed out by adsorption of Pb layers. Therefore, we first show in Fig. 1(a) a LEED pattern of the clean Si(557) surface. Instead of a homogeneous step distribution with an average terrace length of $5\frac{2}{3}$ atomic units (a_0=3.32 Å) in the [$\bar{1}\bar{1}$2] direction, separated by monosteps (3.1 Å), bunching of three units into larger (111) and (112) facets leads to drastic surface reconstructions. Thus, the unit cell amounts to 17 lattice constants, a_0, as obvious from the 16 diffraction spots between the integer order spots. The seventh-order and half-order spots stem from (7×7) and (2×1) reconstructions of the (111) terraces and of the (112) facets, respectively. The (7×7) spots are sharp along the terraces, which indicates good crystalline quality but are streaky normal to the step direction. This is not only a sign for a missing or very small correlation of the (7×7) domains on adjacent terraces. The absence of more round superstructure spots is also a sign for a homogeneously stepped surface, i.e., the absence of facetting of the surface into step bunches and large (111) terraces. This is important for the macroscopic transport studies described below. Further details about the clean surface can be found in Refs. 18–21.

The deposition of multilayers of Pb at temperatures below 100 K is shown in Figs. 1(b) and 1(c). After deposition of three Pb layers on Si(557) at 70 K [Fig. 1(b)] a clear LEED pattern with spots elongated in azimuthal direction is seen. Although the background is comparably high, the (111) texture with an azimuthal broadening around ±7° is clearly visible. As evident from this LEED picture, the Pb layer is nanocrystalline. The spots separations correspond very closely to the lattice constant of a pure Pb(111) layer. Since no signs of the original Si(557) are visible, it is likely that the layer is closed. More direct evidence is provided below by the transport measurements. From previous studies we know that beneath these layers the original step structure is unaltered. It is only modified by annealing to temperatures above 620 K. In this study the layers were never annealed above room temperature. Surprising is the fact that already the three monolayer thick film shows no sign of anisotropy any more in LEED. Both the crystalline growth and the lack of anisotropy are remarkable since the lattice constant of Pb is 8.8% smaller compared to Si. This is in contrast to Si(111), where the first four Pb layers grow as amorphous layers but the system switches back to crystalline layer-by-layer growth at higher coverages.[14] In fact, crystalline layer-by-layer growth starts from the first monolayer on Si(557) (for direct evidence, see the transport measurements below) and growth remains crystalline for thicker layers. This means that there must be an efficient mechanism for strain reduction at the steps of the vicinal surface in order to compensate the large lattice mismatch of Pb, which forms a moderately strong chemical bond, i.e., the Pb layer cannot float on the Si surface such as physisorbed layers.

These statements are corroborated by results of further adsorption of Pb. With the higher thickness, the crystalline islands get larger and better oriented along the Si symmetry directions but the general texture remains. A LEED pattern of 6 ML Pb absorbed on Si(557), again at a surface temperature of 70 K, is shown in Fig. 1(c). The average lateral grain size of the crystallites, deduced from the full width at half

maximum (FWHM) of radial scans through the Pb(01) spot [8% of the surface Brillouin zone, cf. with Fig. 1(d)], is around 5 nm (12 a.u.). It is thus larger than the average width of the (111) facets of the Si(557) substrate, i.e., the (112) facets are partly overgrown by crystalline Pb(111) islands with isotropic surface layers. This is in agreement with a previous SPA-LEED study, revealing an almost identical growth mode if postannealing above 280 K is avoided. The only signature left of the step structure for crystalline Pb films is a tilt of the Pb film by around 1° with respect to the (111) direction.[22] In fact, the crystallinity of the topmost layer(s) of the 6 ML film as well as the amount of azimuthal broadening of around ±4° is practically identical to Pb films with the same thickness on Si(111) substrates.[14] This comparison proves that a thickness of six Pb layers (or less) is able to completely shield the influence of the interface on the growth of further Pb layers, and to effectively compensate any strain induced by the substrate within this layer thickness.

This essentially means that there should be no difference in the properties for additional Pb layers grown on Si substrates with different surface morphology. Since LEED probes geometric properties of the topmost layers only, this hypothesis can be tested more sensitively by a method probing the crystallinity of the entire film structure, including interface and surface effects. Here we use dc electric transport for this purpose. Indeed, this type of measurement provides a higher sensitivity to anisotropies in growth of ultrathin layers and reveals differences due to anisotropies up to at least 10 ML, as shown by us recently.[23] Here we want to concentrate on the layer dependent information contained in the dc transport properties during growth.

B. Bulk and surface dominated transport regimes

For this purpose, we monitored the conductance during evaporation along different crystallographic directions and compared these data with Pb/Si(111). The data of the Pb/Si(111) system were taken from Pfennigstorf *et al.*[24] Since the geometries in their and our measurements were almost identical, the absolute values can be compared directly.

Figure 2(a) shows the conductance measured during adsorption of Pb at 70 K substrate temperature along (circles, $[1\bar{1}0]$ direction) and perpendicular to the steps (diamonds, $[\bar{1}\bar{1}2]$ direction). The low coverage regime is plotted separately in Fig. 2(b). The superimposed small but characteristic oscillations with monolayer periodicity are due to size effects of the Pb films which will be discussed separately in the next subsection. They are, together with the low percolation threshold, the clearest indication of an approximate layer-by-layer growth of Pb layers. The appearance of these characteristics is neither strongly dependent on the deposition rate nor on the substrate temperature in the range 15–100 K.

After deposition of around 0.5 ML Pb, conductance G raises significantly above the conductance of the substrate (≈ 10 μS) both parallel and perpendicular to the step direction. This percolation threshold is close to the theoretical value for random adsorption and indicates that only one Pb layer but no second layer or even three-dimensional clusters,

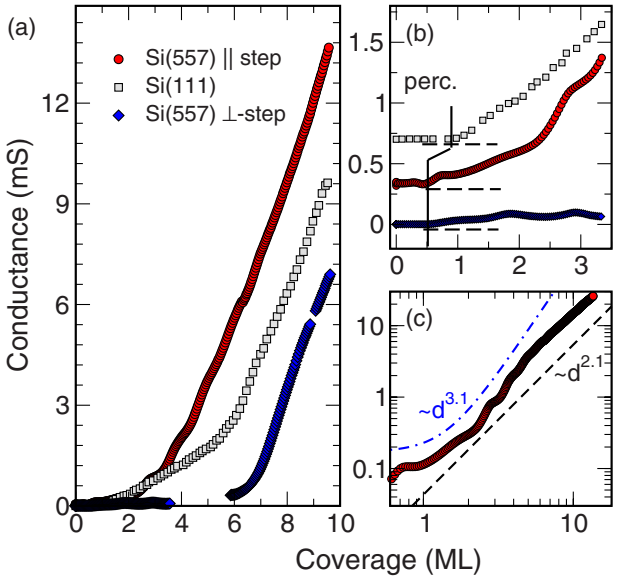

FIG. 2. (Color online) (a) Conductance, G, during Pb evaporation on Si(557) at 70 K measured in various directions: $G_\parallel$ parallel to Si steps (○,red), i.e., along the $[1\bar{1}0]$ direction, $G_\perp$ across the step direction (◇, blue), and on Si(111) (□,gray, data from Ref. 24). (b) Magnification of the low coverage part. The curves are shifted for better visibility. The dashed lines denote zero conductance. The percolation threshold (perc.) depends on the substrate orientation. (c) Log-log plot of $G_\parallel$. The regime up to 5 ML follows a const.$+d^{3.1}$ behavior while above the conductance varies as $d^{2.1}$ (dashed). For better visibility both fits are shifted. For further details see text.

is formed at these low coverages. As Pb is deposited further, the conductance $G_\parallel$ along the steps shows very different behavior compared to $G_\perp$ normal to the steps. Neglecting the conductance oscillations just mentioned in a first step, $G_\parallel$ increases with varying but characteristic functional dependencies on layer thickness, d. While above 5 ML the conductance varies quadratically with d, in the low coverage regime the data are reasonably well described by $G_\parallel \propto d^3$ as shown in Fig. 2(c). The constant introduced there is the residual substrate conductance. On the contrary, the conductance $G_\perp$ measured across the steps remains significantly lower than $G_\parallel$ and increases linearly with d (see also Fig. 4 bottom), i.e., the conductivity $\sigma_\perp \sim G_\perp / d$ remains constant up to 6 ML. Above 7 ML the increment as a function of d is approximately the same parallel and perpendicular to the steps and reflects the isotropy already found with LEED for the growth of further crystalline layers in this coverage regime (cf. Fig. 1). For thinner layers, however, the apparent isotropy of layers found with LEED is not reflected in the conductance data. This is an example where electronic and geometrical properties do not correspond with each other.

Before we try to give an explanation for this discrepancy, we first want to estimate typical elastic electron mean-free path, λ, taking data from angle-resolved photoelectron spectroscopy[8] and from magnetotransport measurements[23] on crystalline Pb multilayer structures. From these data we determined the Fermi velocity (averaged over all subbands) to be $v_F \approx 1 \times 10^6$ m/s. In Ref. 23 was found to be

$\tau_0 \approx 5 \times 10^{-15}$ s almost independent of layer thickness. Thus the elastic mean-free path is of the order of $l_0 \approx 5$ nm, which corresponds to the average lateral size of the crystallites determined with LEED at 6 ML. This means that λ is always much larger than the layer thickness at least up to 10 ML, the thickness range investigated here. Consequently conductance is largely determined by interface properties but also by changes in the electronic band structure, as explained in more detail below.

Indeed, the nonlinear dependence of $G_\parallel$ with increasing coverage, in particular, in the regime below 6 ML, points toward surface related scattering of electrons. According to Refs. 25 and 26 the conductivity is predicted to follow a power law $\sigma \sim d^\alpha$ caused by elastic electron scattering at the interface roughness, if $d \leq \lambda_0$, which is fulfilled here as just demonstrated. The exponent α was found to be around 2.1 for metals and typical metallic electron concentrations down to a minimal thickness of approximately 10 Å.[25,26] Recently, Vilfan *et al.*[27] have shown that this power law is modified to a $\sigma \sim d^{\alpha-1}$ behavior by the quantized electronic structure and the corresponding increase in the density of states at the Fermi energy with increasing film thickness. As obvious from the log-log plot in Fig. 2(c), the conductance ($G_\parallel \sim \sigma \times d$) increases as a function of d with an exponent close to 2, and thus follows perfectly this modified power law for a layer thickness between 5 and 15 ML. Below 5 ML the exponent is slightly higher. Best agreement was obtained assuming an const.$+d^{3.1}$ background. The offset stems from the residual conductance of the substrate (around 10 μS), as mentioned. Indeed, as analyzed in detail by Calecki *et al.*[25,26] higher exponents are expected if the number of occupied subbands (induced by quantum well states) is extremely low. Therefore, the experimentally found thickness dependence of $G_\parallel$ is clearly dominated by interface scattering. As it turned out, it is even semiquantitatively consistent with the results from free-electron-gas models used in Refs. 25 and 26 for the direction parallel to the steps, although anisotropy was not considered there.

This is clearly different for the conductance $G_\perp$ in the direction normal to the steps, where a linear increase up to 7 ML is seen. Such a behavior is expected within a Drude model for $\lambda \ll d$. This assumption, however, would be incompatible with the findings for $G_\parallel$ since interface scattering at rough interfaces cannot be that anisotropic. It is also incompatible with the conductance oscillations seen as a function of layer thickness. Therefore, the mechanism perpendicular to the steps that reduces the conductance for these Pb layers far below the value in parallel direction and causes a modified thickness dependence must be directly related to the electronic transmission probabilities in the direction normal to the steps. Indeed, we found recently in an experiment on a single Pb wire with monolayer height an approximately tenfold increase in resistance per unit length when a substrate step was crossed by the wire.[28] We therefore conclude that the strong electron scattering normal to step edges is not only the reason for the reduced conductance in this direction but that the linear dependence of $G_\perp$ on layer thickness also reflects the thickness dependent change in electronic transmission probability in this direction. As soon as the thickness exceeds 6 ML the steps are again screened for all additional layers and the increment of conductance turns back to close to isotropic.

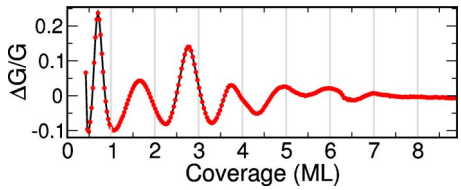

FIG. 3. (Color online) Relative change in conductance $\Delta G/G$ along the step direction. In order to visualize qualitatively the superimposed oscillations on the conductance curve in Fig. 2(a) d^3 and d^2 background was subtracted from the low and high coverage regime, respectively. Only above 5 ML the maxima coincide with the monolayer calibration. Details of the low coverage regime (1–4 ML) are shown in Fig. 4.

Finally, we compare our results on Si(557) with those on isotropic Si(111). Similarly to $G_\perp$, two linear regimes can be discriminated. Furthermore, faint oscillations were seen only for coverages above 7 ML.[24] The linear increase in the conductance in the low coverage regime for Pb/Si(111) was explained by electron scattering which is limited by bulk defects even in these ultrathin layers rather than by an enhanced interface scattering.[11] This conclusion is compatible with the amorphous film growth for Pb/Si(111) up to 4 ML.[14] The threshold for recrystallization of Pb/Si(111) sets in around 6 ML (Ref. 24) and conductance oscillations were found only in the crystalline regime. The conductance measured for multilayers on Si(111) above 6 ML has the same slope as both $G_\parallel$ and $G_\perp$ on Si(557), i.e., in the isotropic crystalline regime we find the same conductive properties on Si(557) and Si(111). However, there is a clear "memory" effect for the properties of the first six monolayers. On the Si(557) surface it was identified as being due to the step induced anisotropy. On Si(111) it is caused by the amorphous interlayer. The memory effect on Si(111) clearly indicates that this amorphous interlayer is not recrystallized by adsorption of additional layers. Otherwise the multilayer conductance should be much closer to $G_\parallel$. In any case, the reappearance of crystalline growth, here demonstrated by identical values of differential conductance above 6 ML of Pb, clearly indicates that appropriate interlayers, even of the same material in our case, can be used in order to efficiently reduce stress effects at the interface in heteroepitaxial systems.[13,17]

C. Classical size and quantum size effects

We now return to the conductance oscillations superimposed on the general trends discussed so far. In order to accentuate these oscillations first in $G_\parallel$ more clearly, we subtracted a smooth function proportional to d^3 up to 6 ML and to d^2 for higher coverages from $G_\parallel$ according to the considerations described above. The difference ΔG divided by $G_\parallel$ is plotted in Fig. 3. This plot reveals several intriguing features and supports the model of a step induced stress compensation: first, incipient with the first monolayer, oscillations are seen up to 8 layers. Second while above 5 ML the oscillation maxima coincide with our monolayer calibration, the pronounced peak structure below this coverage is clearly out-of

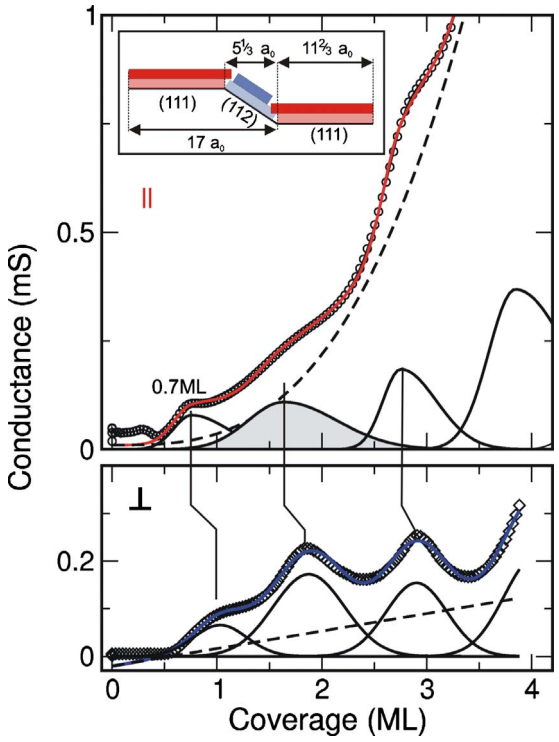

FIG. 4. (Color online) Conductance measured parallel (○, top) and perpendicular (◇, bottom) to the Si(557) steps at 70 K. Dashed lines indicate the continuous increase in conductance neglecting the discrete layer-by-layer growth. The difference between measured data and the dashed lines is plotted at the bottom. Vertical lines mark positions of maxima. The inset shows a simplified growth model of the first two Pb layers on Si(557) deposited at 70 K. Please note, the oscillations are not normalized contrary to those shown in Fig. 3. For details, see text.

phase, i.e., the maxima appear before the layers are completed. Third, as will be discussed in context with Fig. 4, the shift of the maxima with respect to complete layers depends on the crystallographic direction in the coverage regime between 1 and 4 ML, i.e., in the direction across the steps, the maxima in conductance concur with the completion of individual Pb layers at all coverages. Fourth, amplitudes and widths of the oscillations in $G_{\|}$ vary nonmonotonously with layer thickness.

The oscillations can be associated with oscillating interface roughness but also with quantum size effects (QSE) of the Pb film structure, depending on the transport regime and the layer thickness. In the regime, where surface scattering represents a large contribution to the electrical resistance ($\lambda > d$), surface effects can be incorporated via a roughness dependent reflectivity. This so-called CSE can be described quantitatively by the Fuchs-Sondheimer model and the oscillations in the high coverage regime are induced by the periodic variation in the reflectivity factor.[15,16,29] The gradual damping of the oscillations, as seen in Fig. 3, reflects the increasing global roughness, i.e., a less and less strict layer-by-layer growth as a function of layer thickness. In the low coverage regime, however, this classical approach by Fuchs-Sondheimer is inappropriate. In addition, the quantized electronic structure of the film needs to be considered and QSE are expected. For a layer-by-layer growth and a ballistic transmission of the electrons along the film, each new layer results in a new subband, together with relaxations of the already existing subbands.[27] These relaxations lead to variations in the effective band filling, i.e., to dominant *p*- or *n*-type conductance as a function of layer thickness, as obvious from the alternating sign of the Hall resistance,[27] which, however, is not visible in a dc conductance measurement. Although this model is based on *ab initio* calculations for free-standing Pb films,[27] and details of the interaction with the interface may modify the transport properties quantitatively, particularly of the first layer, this subband model should remain qualitatively valid for the first few layers. It means that a new transport channel is opened when the layer starts to be contiguous. Hence the conductance should increase strongly when the percolation threshold of a new layer is reached and should quickly form a new plateau of conductance by further increase in coverage. This phenomenon will be repeated for each layer so that again oscillations with monolayer periodicity are expected but with maxima that do not necessarily coincide with the completion of individual layers, in agreement with our findings. With increasing thickness above five monolayers reduced band splitting and increased overlap of bands seem to modify this simple picture[17] but this range of layer thickness was not considered in detail here. In any case, it is obvious from this short discussion that both CSE and QSE contributions must occur simultaneously in the very thin Pb layers under investigation here, and that separation of these effects may be difficult.

These considerations were taken as a basis in order to describe the conductance curve quantitatively, shown in Fig. 4. Taking first $G_{\|}$, there appears indeed a plateau shortly after the onset of conductance around a coverage of 0.7 ML, which is compatible with QSE. Similarly, the strong and nonmonotonous changes in amplitudes and half widths of the oscillations are hard to be explained by CSE. The model of ballistic transport channels is also to some extent supported by the fact that the amplitudes for the modified Gaussian functions are around the conductance quantum $G_0 = 77\ \mu S$. However, this value depends on the procedure of determining the smooth background function, which was subtracted. It is therefore quite uncertain.

However, both QSE and CSE cannot explain the position of the maxima before layers are completed. It is likely that they are of kinetic origin. Indications for anisotropic growth of Pb is seen already in Fig. 2(b). While the percolation for Pb on Si(111) is around 0.8 ML,[11,24] on Si(557) already around 0.5 ML transport sets it along the step direction. According to the oscillations shown in Fig. 4 the maximum of the conductance along the step direction is around 0.7 ML, which is in good agreement with the fraction of the Si(557) surface covered by (111) facets $[(9+2\frac{2}{3})/17 = 0.68$, see also inset in Fig. 4]. From our experiments with annealed layers of Pb on Si(557) it is well known that Pb adsorption at the step edges is less favorable than on the terraces so that steps are only covered after saturation of the (111) terraces.[18] Since the step structure is the same on both annealed and nonannealed surfaces, we expect that this chemical quantum effect (adsorption with different coordination to the substrate) is similar here. This means that the (112) facets be-

come fully occupied only after the (111) terraces are filled. The selectivity is of course reduced with increasing layer thickness so that the phase difference shrinks with increasing number of layers, as observed. This scenario directly explains, why in $G_{\perp}$ the oscillation maxima appear always at the completion of physical monolayers, in contrast to $G_{\parallel}$. The inset shows only a simplified scenario for the first two monolayers to elucidate the growth of Pb islands with different substrate step densities at the interface. A different growth mode is found for thick layers,[22] where relaxation take place and larger but still inclined crystallites are formed, which were seen by a weak shoulder in their radial scans through first-order spots. The sizes of the tilted crystallites, depending on kinetics, e.g., evaporation rates, etc., and turn out to be smaller in our experiments, as a splitting in the radial scans through the first-order Pb reflexes [cf. Fig. 1(d)] were not clearly resolvable.[30]

For the variation in oscillation amplitudes as a function of film thickness, the formation of standing waves at a layer thickness corresponding to multiples of half the Fermi wavelength is an alternative possibility not yet discussed. Since there are n subbands crossing the Fermi level at very thin layers, there is no unique Fermi wavelength and this model is hard to apply quantitatively to only a few atomic layers. Nonetheless, as obvious from Figs. 3 and 4, the second maximum is reduced and broadened, which is expected since QWS can lower the spectral weight at the Fermi energy. There are indications for an even-odd modulation in the amplitudes. A reduction in the fourth maximum, however, is not as pronounced as for the second one since due to damping by the increasing roughness in the films. A 2 ML modulation for Pb films has been found by DFT calculations and also seen in photoemission spectroscopy.[31,32] Similar results have been obtained by Jal/ochowski *et al.*[13] for Pb growth on Si(111)-(6×6)Au. Although the additional interaction with the substrate modifies the electronic state of the first Pb monolayer, even this Pb layer takes part in this modulation, which is compatible with the phase accumulation model for the formation of QWS (Ref. 33) including stress effects.

IV. SUMMARY AND CONCLUSION

In summary, we presented transport measurements during growth of Pb on Si(557) at low temperature. Contrary to growth of Pb/Si(111), size effects were found incipient with the first monolayer and were discussed in terms of a CSE for coverages higher than 5 ML, where the mean-free path of the electrons become comparable with the thickness. In thinner layers both CSE and quantum size effects are present. This interpretation is consistent with results from LEED and recent temperature dependent transport measurements.[23]

Both LEED and transport measurements have revealed that stress effects due to the large lateral lattice misfit between Si and Pb, which cause amorphous growth on nominally flat substrates, is largely compensated by the high step density on Si(557). This finding is interesting as it could be another strategy for growing nanoribbons with metallic signatures by self-assembly.

ACKNOWLEDGMENT

Financial support by the Deutsche Forschungsgemeinschaft is gratefully acknowledged.

[1] T. Kanagawa, R. Hobara, I. Matsuda, T. Tanikawa, A. Natori, and S. Hasegawa, Phys. Rev. Lett. **91**, 036805 (2003).
[2] J. N. Crain, A. Kirakosian, K. N. Altmann, C. Bromberger, S. C. Erwin, J. L. McChesney, J. L. Lin, and F. J. Himpsel, Phys. Rev. Lett. **90**, 176805 (2003).
[3] H. W. Yeom, S. Takeda, E. Rotenberg, I. Matsuda, K. Horikoshi, J. Schäfer, C. M. Lee, S. D. Kevan, T. Ohta, T. Nagao, and S. Hasegawa, Phys. Rev. Lett. **82**, 4898 (1999).
[4] J. R. Ahn, P. G. Kang, K. D. Ryang, and H. W. Yeom, Phys. Rev. Lett. **95**, 196402 (2005).
[5] T. Tanikawa, I. Matsuda, T. Kanagawa, and S. Hasegawa, Phys. Rev. Lett. **93**, 016801 (2004).
[6] C. Brun, I.-Po Hong, F. Patthey, I. Yu. Sklyadneva, R. Heid, P. M. Echenique, K. P. Bohnen, E. V. Chulkov, and W. D. Schneider, Phys. Rev. Lett. **102**, 207002 (2009).
[7] Ph. Hofmann and J. W. Wells, J. Phys.: Condens. Matter **21**, 013003 (2009).
[8] J. H. Dil, T. U. Kampen, B. Hülsen, T. Seyller, and K. Horn, Phys. Rev. B **75**, 161401(R) (2007).
[9] J. H. Dil, F. Meier, J. Lobo-Checa, L. Patthey, G. Bihlmayer, and J. Osterwalder, Phys. Rev. Lett. **101**, 266802 (2008).
[10] O. Pfennigstorf, A. Petkova, H. L. Günter, and M. Henzler, Phys. Rev. B **65**, 045412 (2002).
[11] O. Pfennigstorf, A. Petkova, Z. Kallassy, and M. Henzler, Eur. Phys. J. B **30**, 111 (2002).
[12] M. Jałochowski and E. Bauer, Phys. Rev. B **38**, 5272 (1988).
[13] M. Jałochowski, E. Bauer, H. Knoppe, and G. Lilienkamp, Phys. Rev. B **45**, 13607 (1992).
[14] A. Petkova, J. Wollschläger, H.-L. Günter, and M. Henzler, Surf. Sci. **482-485**, 922 (2001).
[15] K. Fuchs, Math. Proc. Cambridge Philos. Soc. **34**, 100 (1938).
[16] E. H. Sondheimer, Phys. Rev. **80**, 401 (1950).
[17] N. Miyata, K. Horikoshi, T. Hirahara, S. Hasegawa, C. M. Wei, and I. Matsuda, Phys. Rev. B **78**, 245405 (2008).
[18] M. Czubanowski, A. Schuster, S. Akbari, H. Pfnür, and C. Tegenkamp, New J. Phys. **9**, 338 (2007).
[19] A. Kirakosian, R. Benewitz, J. N. Crain, Th. Fauster, and J. L. Lin, Appl. Phys. Lett. **79**, 1608 (2001).
[20] D. H. Oh, M. K. Kim, J. H. Nam, I. Song, C. Y. Park, S. H. Woo, H. N. Hwang, C. C. Hwang, and J. R. Ahn, Phys. Rev. B **77**, 155430 (2008).
[21] R. Zhachuk and S. Pereira, Phys. Rev. B **79**, 077401 (2009).
[22] E. Hoque, A. Petkova, and M. Henzler, Surf. Sci. **515**, 312 (2002).
[23] D. Lükermann, M. Gauch, M. Czubanowski, H. Pfnür, and C. Tegenkamp, Phys. Rev. B **81**, 125429 (2010).
[24] O. Pfennigstorf, K. Lang, H.-L. Günter, and M. Henzler, Appl. Surf. Sci. **162-163**, 537 (2000).

[25] G. Fishman and D. Calecki, Phys. Rev. Lett. **62**, 1302 (1989).
[26] D. Calecki, Phys. Rev. B **42**, 6906 (1990).
[27] I. Vilfan and H. Pfnür, Eur. Phys. J. B **36**, 281 (2003).
[28] J. Rönspies, S. Wießell, and H. Pfnür, Appl. Phys. A (to be published).
[29] C. R. Tellier and A. J. Tosser, *Size Effects in Thin Films*, Thin films Science and Technology Vol.2 (Elsevier, New York, 1982).
[30] Due to the shielding of the sample for low-temperature conductivity measurements, the resolution of our SPA-LEED is limited in this setup.
[31] C. M. Wei and M. Y. Chou, Phys. Rev. B **66**, 233408 (2002).
[32] P. S. Kirchmann, M. Wolf, J. H. Dil, K. Horn, and U. Bovensiepen, Phys. Rev. B **76**, 075406 (2007).
[33] M. Milun, P. Pervan, and D. P. Woodruff, Rep. Prog. Phys. **65**, 99 (2002).